Space charge limitation on the response time of organic photodiodes

Organic Electronics 34 (2016) 218–222

Contents lists available at ScienceDirect

Organic Electronics

journal homepage: www.elsevier.com/locate/orgel

Space charge limitation on the response time of organic photodiodes

Aart Ligthart [a], Gerwin H. Gelinck [a, b], Stefan C.J. Meskers [a, *]

[a] Molecular Materials and Nanosystems and Institute for Complex Molecular Systems, Eindhoven University of Technology, P.O. Box 513, 5600 MB Eindhoven, The Netherlands
[b] Holst Center, 5656 AE Eindhoven, The Netherlands

ARTICLE INFO

Article history:
Received 14 March 2016
Received in revised form
16 April 2016
Accepted 19 April 2016
Available online 29 April 2016

Keywords:
Organic photodiodes
Space charge limited current
Organic photovoltaics
Photo-impedance spectroscopy
Response time

ABSTRACT

The dynamic response of an organic bulk heterojunction photodiode to small changes in applied bias or light intensity is investigated as function of the intensity of a constant background illumination by means of photoimpedance and transient photocurrent measurements. For bias voltages close to the open circuit voltage we find that the response timescale with the square root of the light intensity. The results can be quantitatively explained in terms of a space charge limitation on the photocurrent as predicted by Goodman and Rose (*J. Appl. Phys.* **42**, 2823 (1971)). The relaxation time of the diode at open circuit corresponds to the lifetime of the slowest charge carrier in the diode. This relaxation time is determined by the dielectric constant and the smallest of the two carrier mobilities in the bulk heterojunction. This illustrates the importance of balanced carrier mobilities for obtaining diodes with fast response time at low bias for e.g. imaging arrays.

1. Introduction

Organic photodiodes with a bulk heterojunction between electron donor and acceptor material as active layer, can be used in imaging applications [1–8]. In some applications the diodes are operated without applying external bias. These include charge coupled device (CCD) array detectors, where the absence of applied bias helps to suppress the dark signal [9]. Furthermore organic photodiodes can be applied in self-powered artificial retinas [10,11]. These artificial retinas are used as prosthesis, to restore vision in patients [12–15]. The photodiode needs to generate a voltage that can trigger depolarization of the membrane of a nerve cell in the retina and give rise to a nerve pulse travelling towards the visual cortex. Obviously, in such an *in vivo* application, the photodiode cannot be powered by an external source. These applications raise the fundamental question as to which material properties determine the response time of the photodiode to changes in light intensity at low bias voltages.

The organic semiconductors used in the diodes are characterized by low carrier mobilities ($\mu \ll 1$ cm^2 V^{-1} s^{-1}) and low dielectric constants ($\varepsilon_r \approx 3$–4). The low mobility implies that photogenerated carriers can easily pile up in the diode, while the low dielectric constant means that electrostatic interactions between the charged carriers are hardly screened. Accumulation of photogenerated carriers [16] results in the built-up of space charge that can limit the response of the photodiode. Already in 1970, Goodman and Rose demonstrated space charge limited photocurrents in diodes featuring low mobility semiconductors [17]. For organic photovoltaic diodes space charge limited, steady-state photocurrent was demonstrated experimentally by Mihailetchi et al. [18] DiNuzzo et al. [19] showed that photoconductivity and photocapacitance under alternating electrical bias are space charge limited when organic photovoltaic diodes are operated under high loads, i.e. applying external bias voltages close to the open circuit voltage.

In this contribution we provide experimental evidence for a space charge limitation of the response time of organic photodiodes at bias voltages close to the open circuit voltage. The organization of the paper is as follows. After a brief description of the experimental procedures, we work out theory for describing the dynamical behavior of the bulk heterojunction photodiodes under open circuit conditions. Under illumination and at open circuit, the diode returns to its steady state with a relaxation time that is determined by the materials properties of the bulk heterojunction and the illumination intensity. Assuming that close to open circuit, currents in the diode are limited by space charge, we derive an explicit expression for this relaxation time and its dependence on illumination intensity. Subsequently, we present experimental

* Corresponding author.
E-mail address: s.c.j.meskers@tue.nl (S.C.J. Meskers).

http://dx.doi.org/10.1016/j.orgel.2016.04.032
1566-1199/

photo-impedance data and determine the relaxation time of the diodes under illumination and open circuit conditions. The experimental data confirm the theoretical predictions of the model for space charge limited photocurrent. Finally, we investigate the response time of the photodiode to small alterations in the light intensity and show that for bias voltages approaching the open circuit voltage, the response time converges asymptotically to the relaxation time determined from photo-impedance measurements. The results indicate that under the conditions chosen, the response time of the diodes is essentially determined by the type of carrier (electrons or holes) with the lowest mobility. Hence dynamical measurements on organic photovoltaic diodes can provide information on the mobility of the 'minority' charge carrier that cannot be accessed easily by static electrical current-voltage characteristics that are mainly determined by the type of charge carrier with the highest mobility.

2. Materials and methods

The diodes under study consist of a bulk heterojunction of poly [*N*-9′-heptadecanyl-2,7-carbazole-alt-5,5-(4′,7′-di-2-thienyl-2′,1′,3′-benzothiadiazole)] (PCDTBT) and [6,6]-phenyl-C_{61}-butyric acid methyl ester (PCBM) deposited from chlorobenzene solution with polymer: fullerene weight ratio of 1:4. The thickness of the bulk heterojunction was 300 nm. This thickness is suboptimal with respect to quantum efficiency but facilitates charge transport studies. Molybdenum oxide is used as anode and a LiF layer (3 nm) covered by a thin Al layer as semi-transparent cathode. Under AM1.5 like illumination conditions, the estimated photovoltaic power conversion efficiency amounts to 1%, with a fill factor of 0.3. Steady-state photocurrent–voltage (*J-V*) measurements were performed using a semiconductor analyzer and a continuous wave HeNe laser as light source (wavelength $\lambda = 543.5$ nm, maximum power density 125 mW/cm^2, beam diameter 1 mm). Light intensities were determined using a calibrated Si photodiode. The intensity of illumination was varied using calibrated neutral filters with optical density ranging from 0.16 to 4.08. Negative bias refers to the top LiF/Al contact being charged negative. Photoimpedance measurements under continuous illumination were done using a Solartron SI 1260 impedance analyzer. The amplitude of the ac voltage modulation was set to 10 mV. The response time of the organic photodiode (OPD) to small changes in illumination intensity was recorded under constant background illumination from the HeNe laser using modulated green light from a fast LED (Kingbright L-7104VGC-H green). The LED output was modulated into a triangular signal with a repetition frequency of 173 Hz using a function generator. The maximum intensity of the LED was 0.01 mW/cm^2, well below the intensity of the background illumination.

3. Theory

A photodiode under continuous illumination connected to an electric power source/sink is, in the thermodynamic sense, an open system out of equilibrium. In the limit of applying a very high external load to the diode under illumination, the diode is essentially operated under the open circuit condition. In this condition, it can be shown that the diode adopts a steady state [29]. After a small perturbation, the diode should return to its steady state with a characteristic time constant, the relaxation time, which is determined solely by diode parameters and independent of the external circuitry. Below we show that by considering the space charge limitation on the built-up of charge carriers in the diode under illumination, one can derive an expression for this relaxation time.

When the hole and electron mobility in a photodiode are unbalanced, e.g. $\mu_h << \mu_e$, then the charge carrier with the lowest mobility will accumulate near its extracting contact while the diode generates a photocurrent under illumination. This results in a space charge region that limits the photocurrent. According to Goodman and Rose [12] the photoconductance G_p is equal to:

$$G_p = qA\left(\frac{9\varepsilon_0\varepsilon_r\mu_h}{8q}\right)^{1/4} g^{3/4}V^{-1/2} \tag{1}$$

with q the elementary charge, A the active area of the diode, $\varepsilon_0\varepsilon_r$ the dielectric constant, and g the rate of charge carrier generation per unit volume. V is the potential difference over the space charge zone, which we assume to be equal to the difference between the externally applied bias V_{appl} and the open circuit voltage V_{oc} of the diode. The photocapacitance of the diode follows from the width of the space charge zone and equals [14]:

$$C_p = \varepsilon_0^{3/4}\varepsilon_r^{3/4}A\left(\frac{8qg}{9\mu_h}\right)^{3/4}(V)^{3/4}. \tag{2}$$

Under open circuit conditions, the relaxation time of the diode equals C_p/G_p, i.e. the RC time of the diode. Note that at open circuit, the external circuit puts an infinite load on the diode. Because the load and internal resistance are parallel, the total resistance of the diode and external circuitry equals the internal resistance of the diode under conditions close to open circuit. The relaxation time can be expressed as:

$$\tau = \left(\frac{8\varepsilon_0\varepsilon_r}{9\mu_h gq}\right)^{1/2} \tag{3}$$

We note that within this model, Eq. (3) can also be interpreted as the lifetime of the slowest charge carrier. Close to open circuit, the space charge limited relaxation time τ describes the characteristic time needed for internal redistribution of the accumulated minority carrier density when making infinitesimal changes in either light intensity or applied bias.

4. Results and discussion

Fig. 1 shows the *J-V* characteristics of the organic photodiode under illumination. In reverse bias at −2 V, the current density

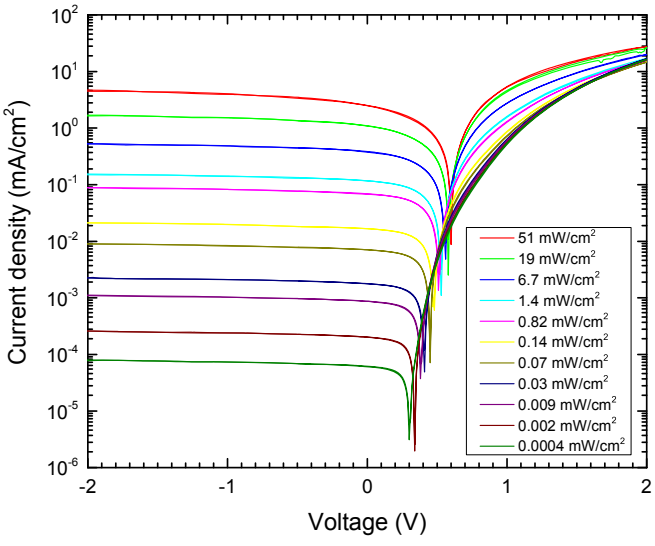

Fig. 1. Current-voltage characteristics of the organic photodiode as function of illumination intensity.

depends in good approximation linearly on the illumination intensity and can be described by a power law $J(-2V) \propto g^{\alpha}$ with $\alpha = 0.95 \pm 0.02$. The external quantum efficiency of the diode for the monochromatic green light is 0.2. The open circuit voltage V_{oc} of the diode is proportional to the natural logarithm of the intensity of illumination with a prefactor of 0.026 ± 0.001 eV. Within experimental error this prefactor equals k_bT/q (0.025 eV), indicating bimolecular free carrier recombination in the organic bulk heterojunction [20–22].

The conductance of the diode under open circuit conditions can be determined by taking the derivative of the current with respect to bias at V_{oc}. We find that the quasi-steady state conductance varies with illumination intensity I according to $G \propto I^{\alpha}$ with $\alpha = 0.74 \pm 0.02$. This is consistent with the prediction for space charge limited conductance $G \propto g^{3/4}$ in Eq. (1). From fitting of Eq. (1) assuming $\varepsilon_r = 4$ we find a mobility for the slowest charge carrier $\mu_h = 1.4 \pm 0.1 \times 10^{-5}$ cm^2 V^{-1} s^{-1} in agreement with previous studies [23,24]. The hole mobility is substantially lower than the mobility of electrons in polymer-fullerene bulk heterojunctions, $\mu_e \approx 10^{-3}$ cm^2 V^{-1} s^{-1} [13,25], or the electron mobility in pure PCBM, $\mu_e > 10^{-3}$ cm^2 V^{-1} s^{-1} [26,27]. This indicates that the assumption of unequal carrier mobility in the Goodman and Rose model is justified.

Further evidence for space charge limited behavior is obtained from impedance measurements. Fig. 2 shows the parallel conductance G_p and parallel capacitance C_p as function of illumination intensity, under application of a DC bias voltage equal to the open circuit voltage under the particular illumination intensity used. The value for the open circuit voltage pertaining to the intensity of the illumination applied in the impedance measurement was determined prior to the impedance measurement by quasi-static current-voltage scans under the same illumination conditions. The dependence of the alternating current conductance and capacitance close to V_{oc} on the intensity can be described as $I^{3/4}$ and $I^{1/4}$, in agreement with previous photoimpedance measurements on organic photodiodes [14,28]. The $I^{3/4}$ and $I^{1/4}$ intensity dependencies agree with the predictions from Eqs. (1) and (2). Because Eqs. (1) and (2) are compatible with bimolecular recombination of free carriers [29], the measured intensity dependencies of open circuit voltage, photoconductance and photocapacitance are consistent. We conclude that the current through the organic photodiode close to V_{oc} is space charge limited.

From the measurements of parallel conductance and capacitance we can calculate the relaxation time of the diode to changes in applied potential near V_{oc}. The calculated C_p/G_p time is illustrated in Fig. 3. It ranges from ~10 to 200 μs, and it follows the predicted $\tau_{RC} \propto g^{-1/2}$ behavior (Eq. (3)).

We now focus on the measurement of the response of the photodiode to changes in illumination intensity. The challenge here is to characterize a response that depends nonlinearly on the light intensity for bias voltages close to the open circuit voltage, i.e. $J \propto g^{3/4}$, see Eq. (1). Fig. 4a shows the triangular intensity profile used to perturb the steady-state photocurrent of the organic photodiode under constant background illumination. The perturbation profile has its maximum around $t = 0$ and is symmetric under time inversion. The red line shows the short-circuit photocurrent response of the OPD with a background illumination of 0.24 mW/cm^2 and a maximum pulse intensity of 0.01 mW/cm^2. As can be seen, the measured photocurrent response of the OPD is clearly lagging behind on probe pulse profile. The maximum of the peak photocurrent is delayed relative to the maximum in pulse intensity.

To extract a response time, we separate the photocurrent response in a time-even and time-odd contribution. The even and odd contributions are plotted in Fig. 4b. The response time τ can be determined from the even and odd contributions to the photocurrent, respectively J_{even} and J_{odd} using the relation [30]:

$$\tau = \frac{J_{odd}}{\frac{dg}{dt}\frac{dJ_{even}}{dg}} = \frac{J_{odd}}{\frac{dJ_{even}}{dt}}. \quad (4)$$

Fig. 5 shows the response time for the photodiode determined for four different levels of background intensity, as function of the intensity of the probe pulse. We note that at the lowest background illumination intensity used (0.24 mW/cm^2), the response time

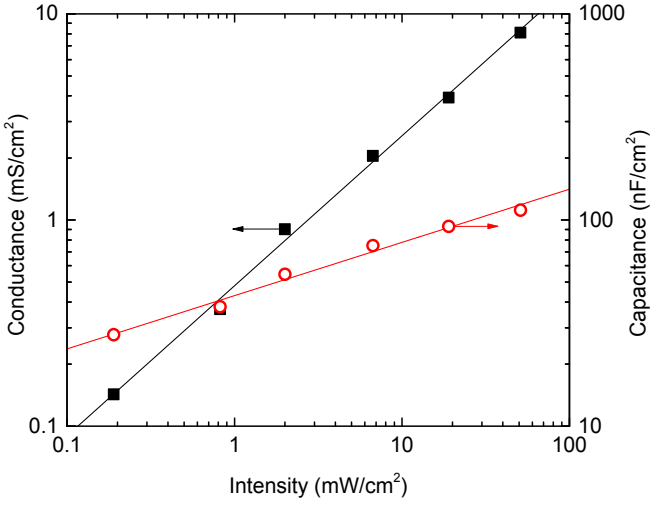

Fig. 2. The parallel conductance (black squares) and parallel capacitance (red open circles) as function of illumination intensity at a frequency of 1000 Hz and a dc bias voltage equal to the open circuit voltage. Solids lines show the fit of a power law function to the data with exponents 0.73 ± 0.02 (conductance, black line) 0.26 ± 0.01 (capacitance, red line). (For interpretation of the references to colour in this figure legend, the reader is referred to the web version of this article.)

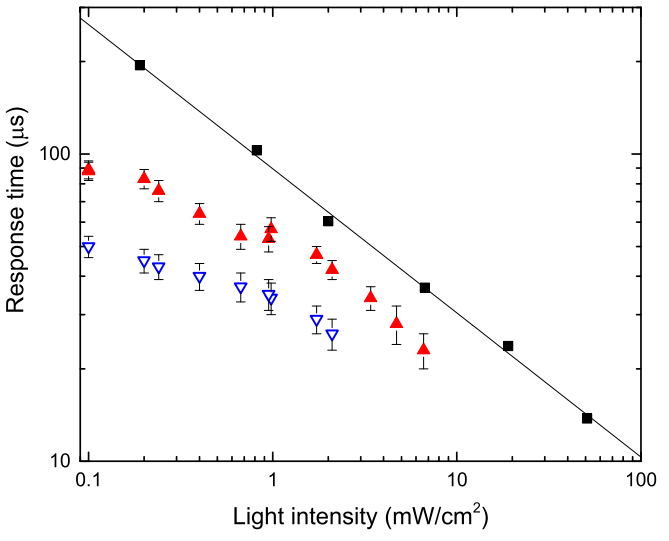

Fig. 3. Response times versus the intensity of constant background illumination. The black squares indicate the R_pC_p time as a function of the illumination intensity determined from the conductance and capacitance measurements plotted in Fig. 2. The black line indicates the fit of a power law I^{α} with $\alpha = 0.47 \pm 0.01$ to the data. The red triangles the show response time to low intensity, modulated probe light (0.01 mW/cm^2) under constant background illumination and a constant applied bias $V_{app} = 0.3$ V. The open blue triangles show the response time to the modulated probe light under short circuit conditions. (For interpretation of the references to colour in this figure legend, the reader is referred to the web version of this article.)

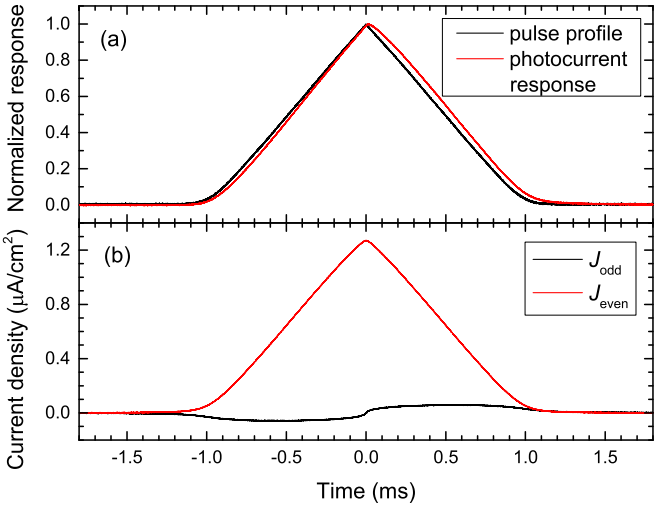

Fig. 4. (a) Black line: pulse profile of the weak probe light with maximum intensity of 0.01 mW/cm^2. Red line: short circuit photocurrent response of the photodiode to the pulse profile under a constant background illumination of 0.24 mW/cm^2. (b) Time-even and time-odd contributions to the short circuit photocurrent response shown in (a). (For interpretation of the references to colour in this figure legend, the reader is referred to the web version of this article.)

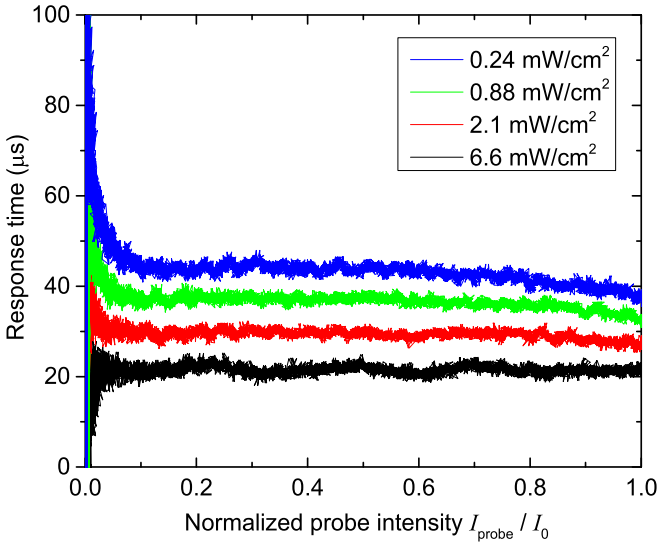

Fig. 5. Response time of the photodiode under short circuit conditions as function of the normalized intensity of the weak probe light, using data as illustrated in Fig. 4 and Eq. (4). Results for four different intensities of constant background illumination are shown (see legend for light intensities applied). Maximum probe light intensity I_0 = 0.01 mW/cm^2.

shows a rapid initial decrease with increasing probe intensity, see Fig. 5. We attribute this initial drop to the filling of deep trapsites by photogenerated charges [31]. At high background illumination intensity, the initial decrease is far less pronounced. The absence of the decrease at low intensities can explained by assuming that the deeper trap states have already been filled by carrier generated by the background illumination. This results in a uniform relaxation time. For low background intensities, not all traps are filled, and carriers generated by the probe light can fill up the empty levels. From the traces shown in Fig. 5, we determine a response from the flat regions between probe intensities of 0.2–0.6 times the maximum probe intensity (0.01 mW/cm^2). For the highest background illumination intensity of 6.6 mW/cm^2, the response time amounts to ~20 μs and is practically independent of the intensity of the probe light. This indicates that the response of the diode to the weak perturbation can be described accurately using a single response time. For lower background illumination intensities, the response time increases. For the lowest background illumination intensity of 0.24 mW/cm^2, the response time amounts to ~45 μs.

Fig. 3 presents the response time of the photodiode to modulated light intensities as function of the background illumination intensity, as determined from traces such as shown in Fig. 5. The blue open triangles represent the optical response times at short circuit. The response time is on the order of tens of microseconds and decreases with increasing illumination intensity. The application of a bias voltage to the diode has a significant influence on the response time. In this study we are interested in the response time under conditions close to open circuit, because under this condition the space charge limited photocurrent model discussed in the introduction makes a prediction. For the range on bias light intensities in Fig. 3 from 1 to 10 mW/cm^2, V_{oc} varies from vary from 0.43 to 0.55 V. Due to technical limitations of the photocurrent detection system used, the bias voltage closest to open circuit conditions for which still reliable current transients could be recorded was $V = +0.3$ V. The red filled triangles in Fig. 3 illustrate the response time for $V = +0.3$ V. As can be seen, the response time to optical perturbation decrease with increasing background illumination and approaches the lifetime of the slowest carrier determined by impedance spectroscopy. At high background intensity, the optical response times are about 0.7 times lower than the corresponding electrical response times. This observation is consistent with the existence of a limit to the response time of the photodiode to a small change in light intensity close to open circuit that scales with the inverse square root of the light intensity.

5. Conclusion

In conclusion, response times for an organic photodiode have been determined experimentally using a constant background illumination. We find that response times for optical and electrical perturbation under conditions approaching open circuit converge to the limit imposed by accumulation of space charge. In this limit, the relaxation time is determined by the dielectric constant and the mobility of the slowest type of charge carrier.

Acknowledgement

We gratefully acknowledge the financial support received from the Dutch Ministry of Education, Culture and Science (Gravity program 024.001.035).

Appendix A. Supplementary data

Supplementary data related to this article can be found at http://dx.doi.org/10.1016/j.orgel.2016.04.032.

References

[1] P.E. Keivanidis, N.C. Greenham, H. Sirringhaus, R.H. Friend, J.C. Blakesley, R. Speller, M. Campoy–Quiles, T. Agostinelli, D.D.C. Bradley, J. Nelson, X-ray stability and response of polymeric photodiodes for imaging applications, Appl. Phys. Lett. 92 (2008) 023304.
[2] T.N. Ng, W.S. Wong, M.L. Chabinyc, S. Sambandan, R.A. Street, Flexible image sensor array with bulk heterojunction organic photodiode, Appl. Phys. Lett. 92 (2008) 213303.
[3] J.C. Blakesley, R. Speller, Modeling the imaging performance of prototype organic x-ray imagers, Med. Phys. 35 (2008) 225–239.
[4] T. Agostinelli, M. Campoy-Quiles, J.C. Blakesley, R. Speller, D.D.C. Bradley, J. Nelson, A polymer/fullerene based photodetector with extremely low dark current for x-ray medical imaging applications, Appl. Phys. Lett. 93 (2008) 203305.

[5] R.A. Lujan, R.A. Street, Flexible x-ray detector array fabricated with oxide thin film transistors, IEEE Elec. Dev. Lett. 33 (2012) 688.
[6] D. Baierl, L. Pancheri, M. Schmidt, D. Stoppa, G.-F. Dalla Betta, G. Scarpa, P. Lugli, A hybrid CMOS-imager with a solution-processable polymer as photoactive layer, Nat. Commun. 3 (2012) 1175.
[7] K.-J. Baeg, M. Binda, D. Natali, M. Caironi, Y.-Y. Noh, Organic light detectors: photodiodes and phototransistors, Adv. Mater. 25 (2013) 4267–4295.
[8] G.H. Gelinck, A. Kumar, D. Moet, J.-L. van der Steen, A.J.J.M. van Breemen, S. Shanmugam, A. Langen, J. Gilot, P. Groen, R. Andriessen, M. Simon, W. Ruetten, A.U. Douglas, R. Raaijmakers, P.E. Malinowski, K. Myny, X-ray detector-on-plastic with high sensitivity using low cost, solution-processed organic photodiodes, IEEE Trans. Electron. Dev. 63 (2016) 197–204.
[9] P. Zygmanski, C. Abkai, Z. Han, Y. Shulevich, D. Menichelli, J. Hesser, Low-cost flexible thin-film detector for medical dosimetry applications, J. Appl. Clin. Med. Phys. 15 (2014) 311–326.
[10] D. Ghezzi, M.R. Antognazza, R. Maccarone, S. Bellani, E. Lanzarini, N. Martino, M. Mete, G. Pertile, S. Bisti, G. Lanzani, F. Benfenati, A polymer optoelectronic interface restores light sensitivity in blind rat retinas, Nat. Photonics 7 (2013) 400–406.
[11] V. Gautam, D. Rand, Y. Hanein, K.S. Narayan, A polymer optoelectronic interface provides visual cues to a blind retina, Adv. Mater. 26 (2013) 1751–1756.
[12] A.Y. Chow, V.Y. Chow, K.H. Packo, J.S. Pollack, G.A. Peyman, R. Schuchard, The artificial silicon retina microchip for the treatment of vision loss from retinitis pigmentosa, Arch. Ophthalmol. 122 (2004) 460–469.
[13] K. Mathieson, J. Loudin, G. Goetz, P. Huie, L. Wang, T.I. Kamins, L. Galambos, R. Smith, J.S. Harris, A. Sher, D. Palanker, Photovoltaic retinal prosthesis with high pixel density, Nat. Photonics 6 (2012) 391.
[14] D. Ghezzi, Retinal prostheses: progress toward the next generation implants, Front. Neurosci. 9 (290) (2015).
[15] L. Bareket, N. Waiskopf, D. Rand, G. Lubin, M. David-Pur, J. Ben-Dov, S. Roy, C. Eleftheriou, E. Sernagor, O. Cheshnovsky, U. Banin, Y. Hanein, Semiconductor nanorod–carbon nanotube biomimetic films for wire-free photostimulation of blind retinas, Nano Lett. 14 (2014) 6685–6692.
[16] F. Arca, S.F. Tedde1, M. Sramek, J. Rauh, P. Lugli, O. Hayden, Interface trap states in organic photodiodes, Sci. Rep. 3 (2013) 1324.
[17] A.M. Goodman, A. Rose, Double extraction of uniformly generated electron-hole pairs from insulators with non-injecting contacts, J. Appl. Phys. 42 (1971) 2823–2830.
[18] V.D. Mihailetchi, J. Wildeman, P.W.M. Blom, Space-charge limited photocurrent, Phys. Rev. Lett. 94 (1) (2005) 26602.
[19] D. Di Nuzzo, S. van Reenen, R.A.J. Janssen, M. Kemerink, S.C.J. Meskers, Evidence for space-charge-limited conduction in organic photovoltaic cells at open-circuit conditions, Phys. Rev. B 87 (2013) 085207.
[20] L.J.A. Koster, V.D. Mihailetchi, R. Ramaker, P.W.M. Blom, Light intensity dependence of open-circuit voltage of polymer: fullerene solar cells, Appl. Phys. Lett. 86 (2005) 123509.
[21] G.A.H. Wetzelaer, M. Kuik, M. Lenes, P.W.M. Blom, Origin of the dark-current ideality factor in polymer: fullerene bulk heterojunction solar cells, Appl. Phys. Lett. 99 (2011) 153506.
[22] G.-J.A.H. Wetzelaer, P.W.M. Blom, Diffusion-driven currents in organic-semiconductor diodes, NPG Asia Mater. 6 (2014) e110.
[23] T.M. Clarke, J. Peet, A. Nattestad, N. Drolet, G. Dennler, C. Lungenschmied, M. Leclerc, A.J. Mozer, Charge carrier mobility, bimolecular recombination and trapping in polycarbazole copolymer:fullerene (PCDTBT: PCBM) bulk heterojunction solar cells, Org. Electron. 13 (2012) 2639–2646.
[24] B. Philippa, M. Stolterfoht, P.L. Burn, G. Juska, P. Meredith, R.D. White, A. Pivrikas, The impact of hot charge carrier mobility on photocurrent losses in polymer-based solar cells, Sci. Rep. 4 (2014) 5695.
[25] M. Morana, M. Wegscheider, A. Bonanni, N. Kopidakis, S. Shaheen, M. Scharber, Z. Zhu, D. Waller, R. Gaudiana, C. Brabec, Bipolar charge transport in PCPDTBT-PCBM Bulk-Heterojunctions for photovoltaic applications, Adv. Funct. Mater. 18 (2008) 1757.
[26] V.D. Mihailetchi, J.K.J. van Duren, P.W.M. Blom, J.C. Hummelen, R.A.J. Janssen, Electron transport in a methanofullerene, Adv. Funct. Mater. 13 (2003) 43–46.
[27] M.P. De Haas, J.M. Warman, T.D. Anthopoulos, D.M. de Leeuw, The mobility and decay kinetics of charge carriers in pulse-ionized microcrystalline PCBM powder, Adv. Funct. Mater. 16 (2006) 2274–2280.
[28] J. Bisquert, G. Garcia-Belmonte, On voltage, photovoltage, and photocurrent in bulk heterojunction organic solar cells, J. Phys. Chem. Lett. 2 (2011) 1950–1964.
[29] See supplemental material for analysis of reverse bias currents and further discussion of Eqs. 1 and 2
[30] T.G.J. van der Hofstad, D. Di Nuzzo, S. van Reenen, R.A.J. Janssen, M. Kemerink, S.C.J. Meskers, Carrier recombination in polymer fullerene solar cells probed by reversible exchange of charge between the active layer and electrodes induced by a linearly varying voltage, J. Phys. Chem. C 117 (2013) 3210–3220.
[31] C.R. McNeill, I. Hwang, N.C. Greenham, Photocurrent transients in all-polymer solar cells: Trapping and detrapping effects, J. Appl. Phys. 106 (2009) 024507.